Mesh adaptation for k-exact CFD approximations

Alain Dervieux, Eléonore Gauci, Loic Frazza, Anca Belme, Alexandre Carabias, Adrien Loseille, Frédéric Alauzet

Mesh adaptation for k-exact CFD approximations

Alain Dervieux, Eléonore Gauci, Loic Frazza, Anca Belme, Alexandre Carabias, Adrien Loseille, Frédéric Alauzet

Abstract:

This paper illustrates the application of error estimates based on k-exactness of approximation schemes for building mesh adaptive approaches able to produce better numerical convergence to continuous solution. The cases of $k = 1$ and $k = 2$, *i.e.* second-order and third-order accurate approximations with steady and unsteady flows are considered.
Keywords: computational fluid dynamics, mesh adaptation, adjoint state

1 Introduction

The purpose of mesh adaptation research is, thanks to an improved accuracy, to be able to compute new phenomena and also to master the numerical uncertain-

Eléonore Gauci · Alain Dervieux
Université Côte d'Azur, Inria, 2004 Route des lucioles, F-06902 Sophia-Antipolis, e-mail: Eleonore.Gauci@inria.fr

Anca Belme
Sorbonne Université, Université Paris 06, CNRS, UMR 719, Institut Jean le Rond d'Alembert Tours 55-65, Bureau 406, Case 162, 4 Place Jussieu, F-75452 Paris, e-mail: belme@dalembert.upmc.fr,

Alexandre Carabias
Société Lemma, 10 rue Melingue F-75019 Paris, e-mail: Alexandre.Carabias@lemma-ing.com,

Loic Frazza · Adrien Loseille · Frédéric Alauzet
INRIA Saclay Ile-de-France 1, rue Honor d'Estienne d'Orves F-91126 Palaiseau, e-mail: Adrien.Loseille@inria.fr,Frederic.Alauzet@inria.fr,

Alain Dervieux · Frédéric Alauzet
Société Lemma, 2000 Route des lucioles, F-06410 Biot, and Inria, e-mail: alain.dervieux@inria.fr

ties which have been up to now unsufficiently controlled. An important strategy is to minimize the approximation error with respect to the mesh. A central question is then to find a good representation of the approximation error. A family of approximations plays a particular role in Computational Fluid Dynamics. The k-exact approximations provide a zero error when the exact solution is a polynomial of degree k. They involve finite elements like continuous and discontinuous Galerkin and ENO finite-volume approximations. Typically, k-exact approximations have a truncation error of order $k+1$.

The purpose of this paper is to adapt mesh using error estimates for a few k-exact approximations in CFD.

We focus on methods which prescribe an anisotropic mesh under the form of a parametrization of it by a Riemannian metric. A Riemannian metric is a continuous symmetric matrix field defined on the computational domain Ω, for example in two dimensions:

$$\mathscr{M} : \Omega \subset \mathbb{R}^2 \to \mathbb{R}^{2^2} \quad \mathbf{x} \mapsto \mathscr{M}(\mathbf{x}) = \mathscr{R}(\mathbf{x})^t \begin{pmatrix} \frac{1}{\Delta\xi(\mathbf{x})^2} & 0 \\ 0 & \frac{1}{\Delta\eta(\mathbf{x})^2} \end{pmatrix} \mathscr{R}(\mathbf{x}).$$

Notation $\mathscr{R}$ holds for a rotation for prescribing mesh stretching directions and $\Delta\xi, \Delta\eta$ for prescribing mesh size in these directions. A mesh obeying these prescriptions is called a *unit mesh* for $\mathscr{M}$. We observe that the very complex and *discrete* thing which is a mesh is replaced by a *continuous* function to be found as the minimum of a numerical error. Then we have to organise a process

$$\text{Metric} \to \text{Mesh and discrete solution} \to \text{Error} \to \text{New metric}$$

which can be thought of as either a pure *discrete* process, or the discretization of a *continuous* process. Let us recall why metrics are particularly adapted to 1-exact approximations. These approximations involve most second-order methods based on continuous P_1 finite-element approximation, namely Galerkin, SUPG, Residual distribution and vertex-centered MUSCL approximations. First, the P_1-interpolation error plays a central role in error estimates. Second, this interpolation error can be converted in terms of the mesh metric. We recall, following [9, 10], the main features of the *continuous metric-based analysis* initiated in several papers like [5, 4, 1]. For a function u defined on the computational domain, we use the continuous interpolation error $u - \pi_{\mathscr{M}} u$ instead of the discrete interpolation error $u - \Pi_{\mathscr{M}} u$:

$$u - \pi_{\mathscr{M}} u = |tr(\mathscr{M}^{-\frac{1}{2}} |H_u| \mathscr{M}^{-\frac{1}{2}})| \quad ; \quad |u - \pi_{\mathscr{M}} u| \approx const. |u - \Pi_{\mathscr{M}} u|, \qquad (1)$$

where H_u is the Hessian of u and $\mathscr{M}$ also denotes a unit mesh for metric $\mathscr{M}$. We consider minimizing:

$$j(\mathscr{M}) = \|u - \pi_{\mathscr{M}} u\|_{\mathbf{L}^1(\Omega_h)}, \qquad (2)$$

and we define as optimal metric the one which minimizes the right-hand side under the constraint of a total number of vertices equal to a parameter N. After solving analytically this optimization problem, we get -solely using the fact that H is a

positive symmetric matrix- the unique optimal $(\mathscr{M}_{\mathbf{L}^1}(\mathbf{x}))_{\mathbf{x}\in\Omega}$ as:

$$\mathscr{M}_{\mathbf{L}^1} = N\left(\int_\Omega (\det(H_u))^{\frac{1}{4}}\right)^{-1} (\det(H_u))^{\frac{-1}{4}} H_u. \tag{3}$$

Knowing the continuous function u, we can derive the continuous optimal metric. In practice, u is solution of a PDE and the whole process of computing u and then deriving the optimal metric is operated by a fixed point iteration involving the generation of a mesh according to the metric, the solution of the PDE on the mesh and the building of a discrete metric.

In this paper, we discuss three types of functional j and the extension to higher-order approximations. For most cases, we propose to evaluate the method by measuring the mesh-adaptive convergence order α, defined by:

$$error = O(N^{-\frac{\alpha}{dim}}), \tag{4}$$

where N is the total number of nodes and dim the dimension of computational domain, and $\alpha = k+1$ for a k-exact approximation.

2 Features-, goal-, norm-oriented formulations

These formulations are presented for the continuous case and applied to the second-order accurate particular case of P^1 approximations on triangles and tetrahedra.

2.1 Feature-based (FB) adaptation

The continuous feature-based anisotropic method (2)-(3) is generally defined by replacing the local interpolation error by the application of the recovered Hessian of the solution times a local mesh size defined by the continuous metric, see [2, 3, 4, 5, 6, 7, 8].

A typical example is the prediction of the sonic boom signature of a supersonic aircraft (see [3] for specific features). Let us consider the C25D geometry of the workshop [24]. We use the Mach number M as sensor, *i.e.* $j(\mathscr{M}) = \|M - \pi_{\mathscr{M}} M\|_{\mathbf{L}^1(\Omega_h)}$. Cuts of mesh and solution are depicted in Figure 1. The FB approach is particularly attractive due to its simplicity and its ability in taking into account physical aspects through the choice of the sensors. However, for systems, the choice of sensors is extremely sensitive.

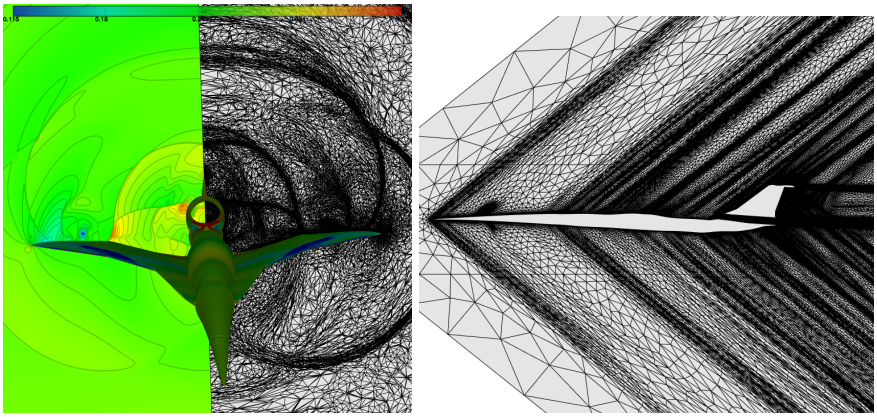

Fig. 1 Lowboom C25 computation with a feature-based mesh adaptation: Cut plane $x = 30$ (left) and on symmetry plane (right).

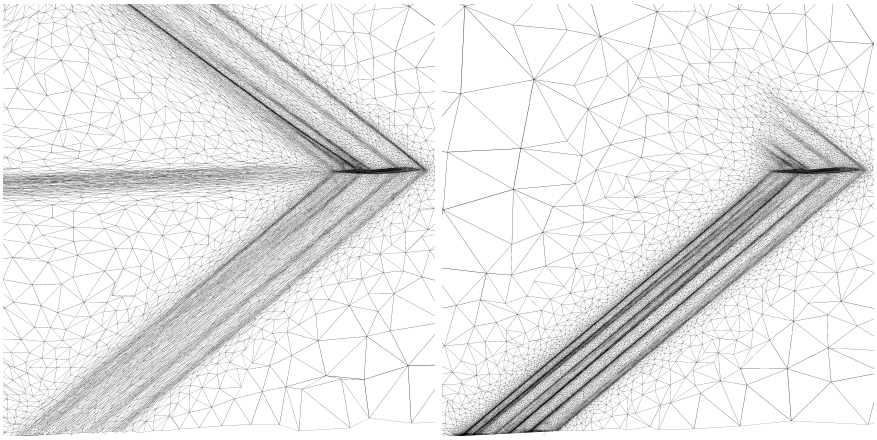

Fig. 2 A typical comparison of feature-based (left) and goal-oriented (right) mesh adaptation for the computation of sonic boom. On left the whole flow is captured, on right, focus is put on the shock structures influencing the boom path at bottom.

2.2 The goal-oriented (GO) formulation

The GO mesh adaptation focuses on deriving the optimal mesh for computing a prescribed scalar quantity of interest (QoI). Many papers deals with *a posteriori* goal-based error formulation to drive adaptivity, using adjoint formulations or gradients, e.g. [14, 13]. We investigate *a priori* based GO formulations for steady and unsteady problems. Loseille *et al.* [11] derived the goal-based error estimate in a steady context for Euler flows, showing that the QoI error estimate is expressed as a

weighted interpolation error on solution flow fields. This leads to an optimal metric computed as a sum of Hessians of Euler fluxes weighted by gradient components of the adjoint state and permits to focus on the capture of important features with respect to the chosen functional, such as sonic boom print at ground, see Figure 2.

2.3 Numerical corrector and norm-oriented (NO) formulation

Given a discrete problem, a mesh (of metric) $\mathscr{M}_h$ and the discrete solution W_h computed with the mesh, we call "numerical corrector" a discrete field W'_h such that the sum $W_h + W'_h$ is a significantly more accurate approximation of the exact solution than W_h. In other words, W'_h is a good approximation of the error. Clearly, W'_h is useful for estimating the error, for correcting it, and for building a norm-oriented mesh adaptation algorithm.

A trivial way to compute W'_h could be to first compute an extremely accurate and extremely costly $W_{h/2^k}$ (k large) solution computed on a mesh $\mathscr{M}_{h/2^k}$ obtained by dividing k times the elements of $\mathscr{M}_h$, and finally to put $W'_h = W_{h/2^k} - W_h$. But the interesting feature of a numerical corrector should be that its computational cost is *not much higher* than the computational cost of W_h. We describe now a corrector evaluation of low computational cost relying on the application of a Defect Correction principle and working on the initial mesh $\mathscr{M}_h$:

$$\Psi_h(W_h + \overline{W}'_{h,DC}) \approx -R_{h/2\to h}\Psi_{h/2}(R_{h\to h/2}W_h) \quad ; \quad W'_{h,DC} = \overline{W}'_{h,DC} - (\pi_h W_h - W_h),$$

where $\pi_h W_h - W_h$ is a recovery-based evaluation of the interpolation error (see [11] for details). The notation $R_{h/2\to h}$ holds for the transfer (extension by linear interpolation) operator from the twice finer mesh $\mathscr{M}_{h/2}$ to the initial mesh $\mathscr{M}_h$, while $R_{h\to h/2}$ holds for the transfer operator from the initial mesh $\mathscr{M}_h$ to the twice finer mesh $\mathscr{M}_{h/2}$. The finer-mesh residual $\Psi_{h/2}(W_h)$ can be assembled by defining the sub-elements of $\mathscr{M}_{h/2}$ only locally around any vertex of $\mathscr{M}_h$. Applications of this method to the Navier-Stokes model can be found in [22]. We present an application with the Euler model used for sonic boom prediction. We consider again the C25 geometry. The important input is the pressure signature at one-body length below the aircraft. Figure 3 depicts the pressure signal and the local error bar, from the non-linear corrector, for a tailored mesh (mesh aligned with the Mach cone) and for adapted meshes. The taylored mesh calculation may seem converged but the corrector remains large. The right-hand side shows a more coherent convergence, with a much smaller corrector.

We can now introduce the NO formulation. We base it on the L^2-norm of approximation error. It consists in the minimization of the following expression with respect to the mesh $\mathscr{M}$:

$$j(\mathscr{M}) = ||W - W_{\mathscr{M}}||^2_{L^2(\Omega)} \quad \text{with} \quad \Psi_{\mathscr{M}}(W_{\mathscr{M}}) = 0. \tag{5}$$

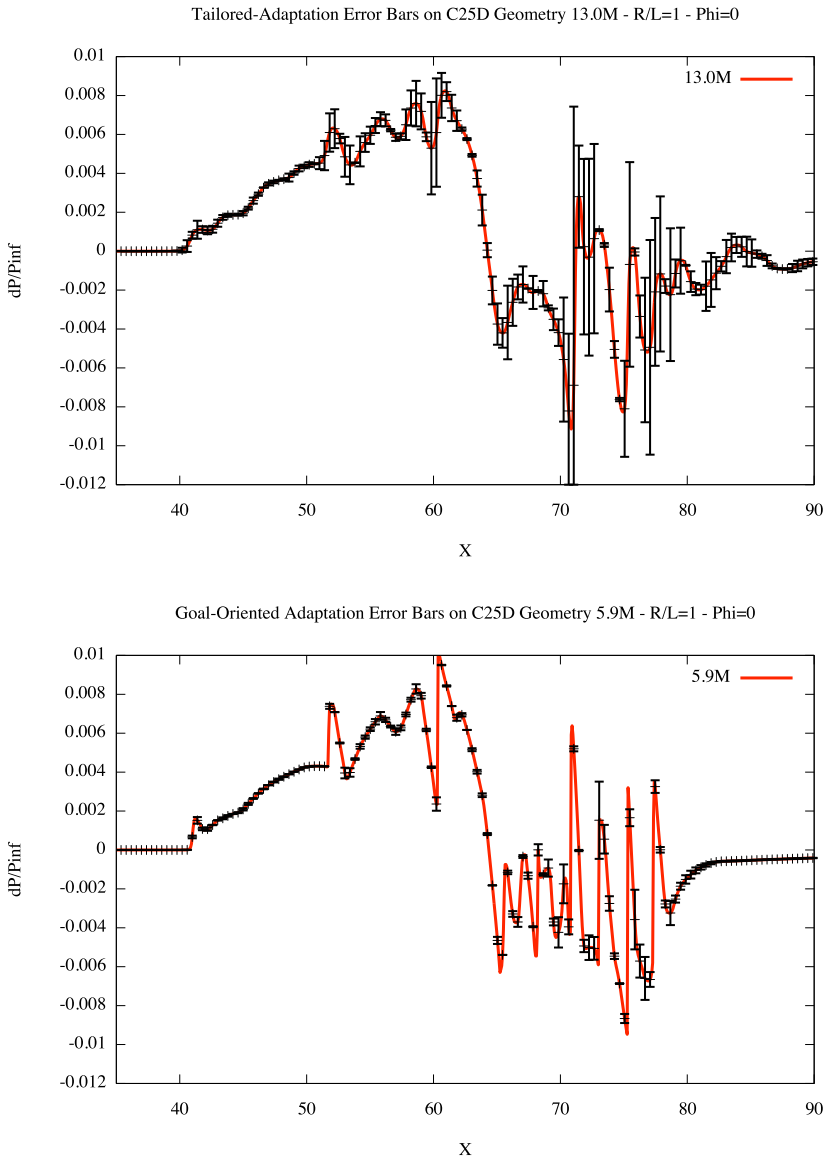

Fig. 3 Flow around a lowboom C25 geometry: Pressure levels (red) and non-linear corrector (black) error intervals for the pressure ($z = 0, y = -C$). Top: on an adhoc tailored mesh. Bottom: on a self-adaptive mesh (right). On right figure, the good convergence is indicated by much smaller intervals.

Introducing $g = W - W_{\mathscr{M}}$, we get a formulation similar to a GO formulation $j(\mathscr{M}) = (g, W - W_{\mathscr{M}})$. The central idea of NO is to replace g by the numerical corrector W_h' as defined in this section. The rest of the NO process follows the GO algorithm with $g = W_h'$. The whole NO adaptation algorithm finally writes:

Step 1: solve state equation for W
Step 2: solve corrector equation for W_h'
Step 3: solve adjoint equation for W^*
Step 4: evaluate optimal metric as a function of W and W^*
Step 5: generate unit mesh for $\mathscr{M}_{opt,norm}$ and go to *Step 1*.

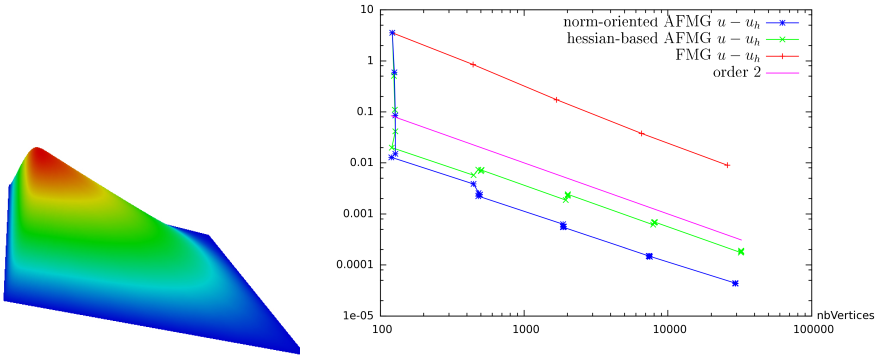

Fig. 4 Elliptic test case of a 2D boundary layer. A comparison between uniform refinement ("FMG"), feature/Hessian-based, and norm-oriented mesh adaptation methods: error $|u - u_h|_{L^2}$ in terms of number of vertices.

In order to give an idea of how this NO works, we consider as *benchmark* a test case from [15] featuring a 2D boundary layer (Figure 4). The Laplace equation is solved with a RHS inducing the boundary layer depicted in the figure. FB and NO mesh-adaptive methods are compared by displaying the convergence curve related to Criterion (4). In abscissae the number of nodes used for computing the discrete solution u_h is shown, and in ordinates the L^2-norm of the aproximation error $u - u_h$ which is measured from the known analytic solution. When the FB method is applied, a tremendous improvement of the error is obtained with 128 vertices, then a uniform element division and further FB adaptation are applied in alternance. While the element division is applied, the error is as expected divided by 4. In contrast, for 512, 1024, 2048,... vertices (abscissae in the figure), the effect of FB adaptation is to *increase* the error, and the second-order convergence is lost. On the contrary, with this test case, each NO mesh-adaptation phase improves (even slightly) the error norm, producing an asymptotic numerical convergence of order two.

3 Estimates for k-exact approximations

Due to their error size and characteristics (dispersion, dissipation), second-order accurate approximations are unable to compute many phenomena. For smooth contexts, high-order methods bring crucial improvements.

3.1 Higher-order (HO) estimates

Main existing HO schemes satisfy the so-called $k-$exactness property expressing the fact that if the exact solution is a polynomial of order k then the approximation scheme will give the exact solution as answer. The assembly of these schemes involves a step of polynomial reconstruction (e.g., ENO schemes), or of polynomial interpolation (e.g., Continuous/discontinuous Galerkin). The main part of the error can then be expressed in terms of a $(k+1)$-th term of a Taylor series where the spatial increment is related with local mesh size. We want to stress that this is the key of an easy extension of metric-based adaptation to HO schemes. We illustrate this with the computation of 2D Euler flows. Considering a triangulation of the computational domain and its dual cells C_i built with triangle medians, the exact solution W of Euler equations verifies (omitting initial conditions):

$$B(W,V_0)=0,\ \ \forall\ V_0\in\mathscr{V}_0=\{V_0\ \text{ constant by cell}\},\ \ \text{with}$$

$$B(W,V_0)\ =\ \int_0^T\sum_i E_i(W,V_0)dt+\int_0^T\int_{\partial\Gamma}\mathscr{F}_\Gamma(W)\cdot\mathbf{n}V_0 d\Gamma dt$$

$$E_i(W,V_0)\ =\ \int_{C_i}V_0\frac{\partial\pi_0 W}{\partial t}d\Omega+\frac{1}{2}\sum_j\int_{\partial C_i\cap\partial C_j}V_0(\mathscr{F}(W)|_{\partial C_i}+\mathscr{F}(W)|_{\partial C_j})\cdot\mathbf{n}d\sigma.$$

Here we denote by π_0 the operator replacing a function by its mean on each cell, $\mathscr{F}$ the Euler fluxes, and the second sum is taken over the cells j neighboring cell i. Let us define a *quadratic Central-ENO scheme* [16, 18]. The computational cost of this scheme is rather large but acceptable for 2D calculations (its extension to 3D is even more computationally expensive). This scheme is based on a quadratic reconstruction on any integration cell C_i using the means of the variable on cells around C_i. Let us denote by R_2^0 the global reconstruction operator mapping the constant-by-cell discrete field into its quadratic-by-cell reconstruction. The CENO scheme writes in short:

$$\text{Find } W_0\ \text{ constant by cell }\ \text{s.t. }\ B(R_2^0W_0,V_0)=0,\ \ \forall\ V_0\ \text{ constant by cell.}$$

A representative functional of goal-oriented error is:

$$\delta j=(g,R_2^0\pi_0W-R_2^0W_0).$$

Lemma 1[19]: *Introducing the adjoint state $W_0^*\in\mathscr{V}_0$, solution of:*

$$\frac{\partial B}{\partial W}(R_2^0 W_0)(R_2^0 V_0, W_0^*) = (g, R_2^0 V_0),\ \forall\, V_0 \in \mathscr{V}_0. \tag{6}$$

we have the following equivalence:

$$(g, R_2^0 \pi_0 W - R_2^0 W_0) \approx \frac{\partial B}{\partial W}(W)(R_2^0 \pi_0 W - W, W_0^*).\square \tag{7}$$

This estimate is typical of a k-exact variational scheme and permits to express the error as a Taylor term of rank $k+1$, rank 3 in our case, with respect to directional mesh size $\delta\mathbf{x}$, which we replace by the power $3/2$ of a quadratic term:

$$\delta j \preceq \sup_{\delta\mathbf{x}} \mathbb{T}(\delta\mathbf{x})^3 \approx \left(\sup_{\delta\mathbf{x}} |\tilde{H}|(\delta\mathbf{x})^2\right)^{\frac{3}{2}} \quad \forall \delta\mathbf{x} \in \mathbb{R}^2. \tag{8}$$

In [19] we fit the second-order tensor $\tilde{H}$ to the third-order tensor $\mathbb{T}$ by least-squares, and the optimal metric is computed in a similar way to the second-order accurate case. An *a priori* better option for accounting higher-order interpolation error, not tested here, is to apply the strategy of [21].

Remark: The *a priori* estimate of Lemma 1 is inspired by the *a posteriori* estimates of Barth and Larson [17] in which the authors explain that the analysis extends to many k-exact approximations of high-order. This is also true for the present *a priori* analysis. In particular, the analogous estimate for a k-exact *discontinuous* P_k-*Galerkin* approximation writes:

$$(g, \Pi_k W - W_k) \approx \frac{\partial B}{\partial W}(W)(\Pi_k W - W_k, W_k^*), \tag{9}$$

where W_k and W_k^* are the DG_k discrete state and adjoint and Π_k the elementwise interpolation of degree k.$\square$

3.2 High-order accurate unsteady mesh adaptation

We illustrate the use of the above estimate (6)-(8) with an application to an unsteady flow. For many propagation phenomena, the discretisation grid (space and time) necessary for a complete representation is very heavy. We consider here an acoustic wave propagation based on the Euler equations.

In order to apply an unsteady mesh adaptation, we adopt the so-called Global-Fixed-Point algorithm [12]. In short, the time interval is divided in n_{adap} sub-intervals. After a computation of state and adjoint on the whole time interval, an optimal space-time metric is evaluated as a set of spatial metrics for each of the time sub-intervals.

In Figure 5, the propagation of a noise from a road (bottom left) to a balcony (near top, right) around an anti-noise wall (middle of bottom) is computed. The functional

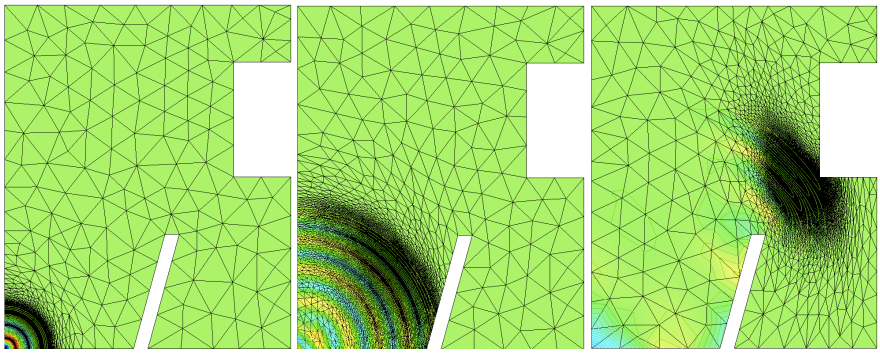

Fig. 5 Goal Oriented unsteady calculation of nonlinear acoustics propagation with third-order goal-oriented adaptation. Pressure at three different time levels and the corresponding meshes.

is the pressure integral on an interval of the balcony. Since a few wavelengths are emitted at the noise source, the mesh adaptation process will concentrate on the part of the wave train which will hit the balcony. This dramatically reduces the region of the computational domain which needs to be refined. With 30980 vertices (mean of the 20 meshes used over the time interval) the resolution is about 10 points per half wave and would require 5 millions vertices if the mesh were a uniform mesh of same maximal fineness. As for Criterion (4), we have measured for this case $\alpha = 2.45$, which is not satisfactory with respect to the theoretical order of approximation, which is 3, but already carries an important improvement with respect to analogous adaptation based on a second-order finite-volume approximation, see [20].

4 Conclusions

The k-exact analysis described in this note allows us to express errors in terms of interpolation errors. This holds for various k-exact approximations like FVM, FEM, DG, ENO. This also holds for three types of adaptation strategies, namely the feature-based, the goal-oriented, and the norm-oriented. Applications with P_1-Galerkin and P_2-CENO approximations are demonstrated. This method can be complemented with a special treatment of singularities, [25], and combined with a FMG process, [23].

Acknowledgements This work has been supported by French National Research Agency (ANR) through project MAIDESC n^o ANR-13-MONU-0010. This work was granted access to the HPC resources of CINES under the allocations 2017-A0022A05067 and 2017-A0022A06386 made by GENCI (Grand Equipement National de Calcul Intensif).

References

1. Agouzal, A., Lipnikov, K., & Vasilevskii, Y. 1999. Adaptive generation of quasi-optimal tetrahedral meshes. *East-West Journal*, **7**(4), 223–244.
2. Alauzet, F., & Loseille, A., 2010. High order sonic boom modeling by adaptive methods. *J. Comp. Phys.*, **229**:561–593.
3. Loseille, A., & Löhner, R., 2010. Adaptive anisotropic simulations in aerodynamics. In *48th AIAA Aerospace Sciences Meeting and Exhibit*, AIAA-2010-169, Orlando, FL, USA.
4. Castro-Díaz, M.J., Hecht, F., Mohammadi, B., & Pironneau, O., 1997. Anisotropic unstructured mesh adaptation for flow simulations. *Int. J. Num. Meth. in Fluids*, **25**:475–491.
5. Dompierre, J., Vallet, M.G., Fortin, M., Bourgault, Y., & Habashi,W.G., 1997. Anisotropic mesh adaptation: towards a solver and user independent CFD. In *AIAA 35th Aerospace Sciences Meeting and Exhibit*, AIAA-1997-0861, Reno, NV, USA, Jan 1997.
6. Vasilevski, Y.V., & Lipnikov, K.N., 2005. Error bounds for controllable adaptive algorithms based on a hessian recovery. *Computational Mathematics and Mathematical Physics*, **45**(8):1374–1384, 2005.
7. Huang, W., 2005. Metric tensors for anisotropic mesh generation. *J. Comp. Phys.*, **204**:633-665, 2005.
8. Frey, P.J., & Alauzet, F., 2005. Anisotropic mesh adaptation for CFD computations. *Comp. Meth. Applied Mech. Eng.*, **194**(48-49):5068–5082.
9. Loseille, A., & Alauzet, F., 2011. Continuous mesh framework. Part I: well-posed continuous interpolation error. *SIAM NUMA*, **49**:1,38-60.
10. Loseille, A., & Alauzet, F., 2011. Continuous mesh framework. Part II: validations and applications. *SIAM Num. Anal.*, **49**(1):61–86.
11. Loseille, A., Dervieux, A., & Alauzet, F. 2015. Anisotropic Norm-Oriented Mesh Adaptation for Compressible Flows. *In: 53rd AIAA Aerospace Sciences Meeting*. AIAA-2015-2037, Kissimmee, Florida.
12. Belme, A., Dervieux, A., & Alauzet, F. 2012. Time Accurate Anisotropic Goal-Oriented Mesh Adaptation for Unsteady Flows. *J. Comp. Phys.*, **231**:19, 6323 6348
13. Yano, M., & Darmofal, D., 2012. An optimization framework for anisotropic simplex mesh adaptation: application to aerodynamics flows. *AIAA Paper*, 2012-0079.
14. Ferro, N., Micheletti, S., & Perotto, S., 2018 Anisotropic mesh adaptation for crack propagation induced by a thermal shock in 2D. *Comput. Methods Appl. Mech. Engrg.*, **331**, 138-158.
15. Formaggia, L., & Perotto, S., 2003. Anisotropic a priori error estimates for elliptic problems. *Numer. Math*, **94**:67-92.
16. Barth, T.J., & Frederickson, P.O., 1990. Higher order solution of the Euler equations on unstructured grids using quadratic reconstruction, AIAA Paper 90-13.
17. T.J. Barth and M.G. Larson. A-posteriori error estimation for higher order godunov finite volume methods on unstructured meshes. In R. Herbin and D. Kröner, editors, *Finite Volumes for Complex Applications III*, pages 41–63. 41 63, 2002.
18. Ivan, L., & Groth, C.P.T., 2014. High-order solution-adaptive central essentially non-oscillatory (CENO) method for viscous flows. *J. Comp. Phys.*, **257**:830-862.
19. Carabias, A., Belme, A., Loseille, A., & Dervieux, A., 2018. Anisotropic goal-oriented error analysis for a third-order accurate CENO Euler discretization. *Int. J. Num. Meth. in Fluids*, **86**:6, 392 413.
20. Carabias, A., 2013. Analyse et adaptation de maillage pour des schémas non-oscillatoires d'ordre élevé (in french). PHD, Université de Nice-Sophia-Antipolis, France.

21. Coulaud, O., & Loseille,A., 2016. Very High Order Anisotropic Metric-Based Mesh Adaptation in 3D. 25th International Meshing Roundtable. *Procedia Engineering*, **163**, 353-365.
22. Frazza, L., Loseille, A., Alauzet, F. & Dervieux, A., 2018. Nonlinear corrector for RANS equations, AIAA conf. 2018.
23. Brèthes, G., Allain, O., & Dervieux, A., 2015. A mesh-adaptative metric-based full multigrid for the Poisson problem, *Int. J. Num. Meth. in Fluids*,**79**-1, 30 53.
24. 2nd AIAA Sonic Boom Prediction Workshop (2017) Grapevine, Texas.
25. E. Gauci, A. Belme, A. Carabias, A. Loseille, F., 2018. Alauzet, A. Dervieux, A priori error-based mesh adaptation in CFD, special issue of *Journal of Methods and Applications of Analysis*.